Journal of Heat and Mass Transfer Research 7 (2020) 143- 154

Semnan University

Journal of Heat and Mass Transfer Research

Journal homepage: http://jhmtr.semnan.ac.ir

Developing a Model for Predicting the Outlet Gas Temperature of Natural Gas Pressure Reduction Stations to Reduce Energy Loss

Saeed Rastegar, Hadi Kargarsharifabad*, Abdollah Khalesi Doost, Nader Rahbar

Energy and Sustainable Development Research Center, Semnan Branch, Islamic Azad University, Semnan, Iran.

PAPER INFO

Paper history:
Received: 2019-12-04
Revised: 2020-06-18
Accepted: 2020-06-19

Keywords:
Regulator;
Natural gas;
Hydrate;
Pressure reduction station.

ABSTRACT

Natural gas stream must be preheated before pressure reduction takes place at natural gas pressure reduction station (PRS). It ensures that the natural gas stream remains above hydrate-formation zone. Heaters are used to prevent this problem. There is no precise method for determining the adjustment points of heaters; and the gas is usually heated to a temperature higher than the required temperature leading to the energy loss in heaters. In the present paper, the outlet gas temperature of regulator was predicted to prevent the energy dissipation by an applied analysis through thermodynamics equations and considering the deviation of natural gas from the ideal gas state using MATLAB software. The prediction of outlet temperature and application of control mechanisms made the temperature close to the standard temperature, so that avoiding the formation of destructive hydrate phenomenon, prevented the dissipation of 7983.7 standard cubic meter of natural gas and reduced 15.29 tone greenhouse gas emissions in a year at the PRS under study. The economic analysis of the proposed system has been carried out using Payback ratio method. The payback period of implementation of this control system is only less than one year. Results of comparison between the measured output temperature and calculated temperature through the software indicated an average difference of 9%.

DOI: 10.22075/jhmtr.2020.19223.1261

1. Introduction

In the past years, natural gas production, transmission and distribution have encountered problems due to the – blocking of pipelines by settling of crystals that were initially thought to be ice crystals. These crystals are in fact natural gas hydrates that can appear at temperatures above the ice formation temperature. The crystals are external compounds that are resulted from the combination of water and some of natural gas ingredients and mainly methane [1]. In order to prevent pipeline clogging, facilities for production, transmission and distribution should be protected from hydration. Gas desiccation is a way to achieve this goal. If this is impossible, the use of hydrate formation inhibitors is recommended [2]. Furthermore, thermodynamic conditions preventing the hydrate formation can be achieved by increasing temperature at a certain pressure or decreasing pressure at a certain temperature [3]. If these conditionsare not possible, the hydrate formation inhibition can be achieved by reducing the water content of gas by drying or using inhibitors [4]. Inhibitors act as the antifreeze. They are generally selected from hydrous extractable solvents that change the fugacity of water and reduce the hydrate formation temperature [5]. The above-mentioned cases delay the hydration formation, but do not inhibit the hydrate formation. To ensure that hydrates are not formed, the outlet temperature of a regulator should be predicted and become close to the standard natural gas temperature (15 ℃) [6, 7].

According to the general equation of gases, the gas temperature decreases by reducing the pressure in the constant volume. Since the natural gas deviates from the

Corresponding Author: Hadi Kargarsharifabad, Energy and Sustainable Development Research Center, Semnan Branch, Islamic Azad University, Semnan, Iran.
Email: h.kargar@semnaniau.ac.ir

ideal gas state, its compressibility factor should be calculated. Several methods have been used to calculate the natural gas compressibility factor [8, 9]. Conducted studies led to a standard method for calculating the natural gas compressibility factor up to 4 MPa in the American Standard Natural Gas Research Circle. The natural gas compressibility factor as well as a state equation were developed and published. The results of above study were published by the American Gas Association (AGA) in 1962 under the title of "Guidelines for calculating natural gas compressibility factor". After revisions, a new state equation was provided for calculating the natural gas compressibility factor by GRI and GERG institutions. The revised method was also completed by - Richard Jacobson using experimental and analytical data [10].

Erfani et al. [11] during a review article, discussed different operations considering applications of gas hydrate. These operations were classified based on both contact of liquid and vapour phases and methods of conducting mass and heat transfer. Rahbar et al. [12] investigated fluid flow and energy separation in a micro-scale Ranque-Hilsch Vortex Tube, numerically. The results showed that fluid flow and energy separation inside the micro-scale vortex tube was quite similar to those of traditional ones. Moreover, it was found that non-dimensional forms of cold temperature difference and refrigerating capacity were only dependent on cold mass fraction. In addition, two correlations were proposed to estimate non dimensional forms of cold temperature difference and refrigeration capacity in the micro-scale vortex tube. Falavand Jozaei et al. [13] the arbitrary high order DG-ADER method applied to analyse the transient isothermal flow of natural gas through pipelines. They simulated two real problems with associated field data. The results showed that highly accurate results can be obtained using the DG-ADER method, even on a coarse grid. Furthermore, the conventional small amplitude oscillations of DG-ADER method did not appear in the transient natural gas flow due to the smoothness of the flow field properties.

The available natural gas pressure decreases in transmission pipelines of pressure reduction stations (PRSs) for various uses including the domestic consumption. At these stations, the gas pressure decreases during an expansion process using the regulators. During this process, because of the lowering of the gas temperature (simultaneously with the decrease in its pressure), owing to the presence of water and some heavy hydrocarbons in the natural gas composition, a two-phase flow is created and causes the hydrate formation and freezing on the outlet of natural gas PRS. The gas must be heated before it enters regulator to ensure that it remains above the natural gas dew point. The heaters of natural gas PRS consume a considerable amount natural gas for preheating. Often applied heat exceeds the amount needed to supply natural gas heating. Therefore, numerous studies have been conducted in recent years [14–19]. In this regard, different control methods have been examined such as determination of parameters affecting the amount of energy consumption and its reduction, the use of solar systems for reducing the fuel consumption, techniques for estimating the amount of consumed energy in different sectors of natural gas PRS and the efficiency of available heaters at these stations, and the replacement of gas heaters with line and electric heaters at the of natural gas PRSs. Rastegar et al. [20] investigated the use of thermosyphon heat pipes for heat transfer from the fire tube to the gas tube. They found that using heat pipes with suitable working fluid and proper filling ratio improves heater efficiency by 13%. Khalili et al. [21] calculated the heat dissipation and heater efficiency of Shahre-kord station. Their calculations indicated that more than 38% of combustion energy was wasted through the exhaust gas pipe over a year. In their research, it was also found that 2% of the energy was lost through the heater surface. In this study also, the efficiency of desired heater was less than 47%. Riahi et al. [22] proposed several solutions to optimize combustion efficiency of installed heaters at Ardabil Station. They could increase the combustion efficiency by 10% and increase the total heat output by 30% through adjusting the flame length related to the combustion chamber, adjusting the air to fuel ratio, and installing damper. Farzaneh-gard et al. [23] reviewed the use of solar systems at Sari of natural gas PRS. They designed an intelligent solar system consisting of a reservoir tank with adequate capacity and a number of flat collectors and determined the best arrangement and optimal number of collectors by calculating the absorbing solar flux in the studied area. Olfati et al. [24] examined a PRS of 20,000 SCMH capacity in terms of both energy and exergy. They showed that seasonal changes over a year contribute to thermodynamic performance of such a PRS, and highest rate of exergy loss (15.33 kW) and exergy destruction (153.85 kW) occurred at the heater exhaust and combustion chamber of the heater, respectively. Also, Olfati et al. [25] in another research, proposed a novel modification on preheating process of natural gas in PRSs to improve energy consumption, exergy destruction and reduction of CO_2 emission. They showed that compared to conventional stations, the modified station at least 33% and 15% reductions in energy consumption and exergy destruction, respectively. They also showed that the performance of two sample stations by implementing the proposed modification, CO2 emission reduced by up to 80% . Based on the literature, a great number of studies have been conducted on preventing hydration formation, freezing the natural gas, as well as natural gas PRS in various fields including the increased efficiency, but to the best knowledge of the authors of the present paper, there is no research on the use of an industrial control system for automatic control of fuel consumption of heaters. The aim of of this study is utilization a proper control system for the heaters of PRS, so that the required amount of heat is applied to natural gas flow. Therefore , the loss of a large amount of energy and also greenhouse gas emissions would be pervented.

2. Theoretical background

2.1. Natural gas PRS; reason and method of heater operation

The extracted gas from gas fields is distributed by main transmission pipelines in Iran after refining operations in refineries. Due to the gas friction along the transmission pipelines and sub-drops in the transmission network, the gas pressure decreases which can be compensated by gas pressure increasing stations. At these stations, gas is compressed and its pressure increases. Gas pressure in main gas transmission pipelines should be within the permissible limits before they reach the distribution station. Gas pressure is from 4800 kPa to 10000 kPa in the main pipelines of intercity gas transmission. For the urban consumption, this pressure should decrease to 1700 kPa at the PRS and 6800 kPa at the Town Border Station (T.B.S) in two steps. The gas temperature also drops due to the pressure drop in the regulator. In cold weather, in which the temperature of inlet gas of station is low (less than 5° C), the temperature becomes less than 0℃ at the outlet of regulator. Therefore, the vapor particles of gas undergo the phase change and become as gas hydrates. This phase change leads to the blocked gas passage sensing lines in the regulator. Gas is heated before the pressure reduction in order to prevent freezing water vapor particles in the gas by reducing pressure. An indirect heat exchanger is the applied heating system for this purpose. These types of heating systems are as sources of horizontal cylinders with spiral tubes that transmit gas through pipes and become warm. In these heat exchangers, the hot fluid containing high thermal energy is the combustion product. Combustion products are results of reaction of fuel-air mixture in the heater stack. A mixture of water and antifreeze is the intermediate fluid in the heater and plays the role of transmitting the thermal energy in a hot fluid to a cool fluid. The mechanism of heat transfer from hot fluid to cold fluid is natural convection. Fig. 1 shows a scheme of an example of these heaters and their various components, known as indirect water bath heaters.

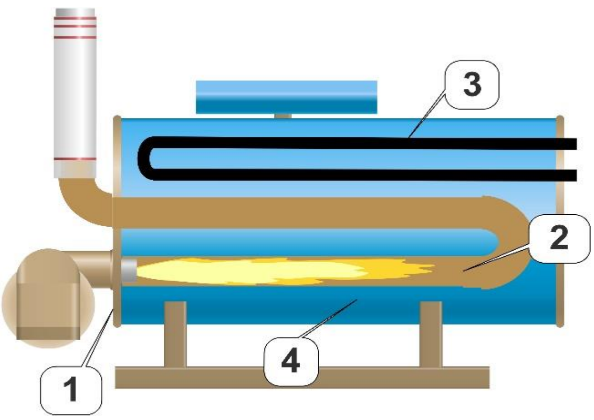

Figure 1. Custom schematic heater in PRS: 1-Heater, 2- Fire tube, 3- Gas tube and 4-Water medium.

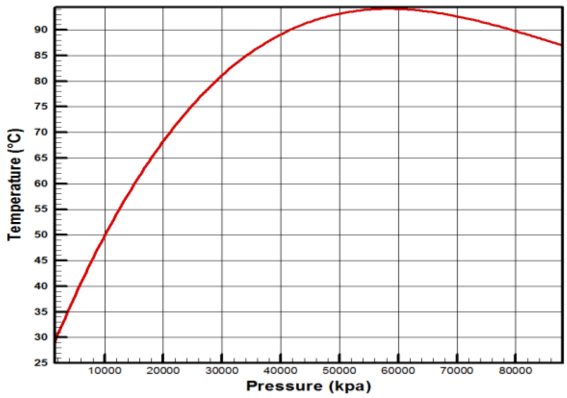

Figure 2. Curve of constant enthalpy for natural gas.

2.2. Thermodynamics of expansion in regulator

In the PRS, the gas pressure decreases up to -1.7 Mpa in a regulator. Joule–Thomson coefficient is usually utilized to find out how properties change during the throttling process as presented in the Equation (1).

$$\mu_j = (\frac{\partial T}{\partial P})_h \tag{1}$$

In general, if gas is at the temperature of T_1 and pressure of P_1 before entering the regulator, and then at the temperature of T_2 and pressure of P_2, the reduced pressure ($P_1>P_2$) may increase or decrease the temperature depending on the sign of Joule–Thomson coefficient.

It is experienced that the pressure drop in regulator decreases the temperature for natural gas in transmission pipelines (Joule–Thomson coefficient is always positive); and this is the reason for using the heater. For the sign of Joule–Thomson coefficient for natural gas, the constant enthalpy graph is studied for gas with common conditions in gas transmission pipelines. For instance, the constant enthalpy diagram of South Pars refinery, which provides the gas of studied station in this paper, is shown in Fig. 2.

Fig. 2 is consistent with our experience with the positivity of Joule–Thomson coefficient because the maximum pressure is about 6900 kPa in gas pipelines; and according to the above diagram, Joule–Thomson coefficient is also positive (ascending graph) for this pressure or higher pressures; and the reduced pressure decreases the temperature. According to Fig.2, when Joule–Thomson coefficient is positive, the higher the pressure drops, the greater the temperature drops. Therefore, it can be concluded that the higher the input pressure to the station, the higher pressure drop in the regulator to reach the pressure to 1700 kPa at the outlet, and consequently, leading to the higher temperature drop. Considering the constant temperature for the inlet gas of station, the higher pressure leads to the greater pressure drop and thus the higher temperature drop and lower output temperature; hence the possibility of hydrating gas would be higher at the outlet and conditions would be more critical. Gas is expanded while passing the regulator at the PRS. The expansion in the regulator is based on the Joule–Thomson process; and the continuity equation and the first law of thermodynamics are according to the Equations (2) and (3) [26]:

$$\left(\frac{dm}{dt}\right)_{c.v.} + \dot{m}_e - \dot{m}_i = 0 \quad (2)$$

$$\dot{Q}_{c.v.} = \dot{m}_e\left(h_e + \frac{V_e}{2}\right) - \dot{m}_i\left(h_i + \frac{V_i}{2}\right) \quad (3)$$

In most cases, the process of throttling occurs so quickly and in a small media, so that there is not enough time and place for the heat transfer. Therefore, the process is carried out steady state and adiabatic-, and no changes occur in the potential energy. Therefore equation (3) is simplified according to the Equation (4):

$$h_i + \frac{V_i^2}{2} = h_e + \frac{V_e^2}{2} \quad (4)$$

As pressure decreases, the gas flow velocity increases after the regulator. In some places, the velocity of gas may quickly reach the critical speed (critical speed is the sound speed in gas at a certain pressure). It is about 427 m/s for the natural gas [6]. If the gas velocity reaches this value, the choke flow condition occurs in the regulator. In order to avoid it, the pipe after the regulator is usually built in a size of two times higher than the previous size while designing the station [27]. The kinetic energy statements can be neglected if:

- This energy is kept equal on both sides.
- Due to the larger diameter of pipe after the regulator than the previous pipe, these energies become approximately equal; and the difference in this energy can be neglected assuming that the volume flow rate is low.

In this case, the steady flow equation will be simplified as the Equation (5):

$$h_i = h_e \quad (5)$$

2.3. Certain data and the missing parameter at the PRS

At the natural gas PRS, there are certain inlet temperature of pressure of station; and the operator does not play any role in their change or adjustment. The outlet pressure of station's regulator should be set to 1.7 MPa (250 PSI), but the temperature of outlet gas is unknown. The gas temperature decreases as the pressure decreases; hence, the gas temperature after pressure reduction must be adjusted in a way that it does not reach the dew point temperature of natural gas, otherwise, liquid droplets emerge in gas and cause the hydrate formation and freezing. Understanding the conditions under which the water vapor in natural gas is condensed plays an important role in design and operation of that system. Natural gas contains one or more condensing components and non-condensable component. If there are certain temperature and pressure changes in the regulator of the PRS, the dew point curve of natural gas can be used to determine areas where the condensation is possible [28].

Two thermodynamic properties are necessary for a simple compressible material in order to determine other thermodynamic properties of material. Therefore, the amount of input enthalpy is calculated according to the inlet temperature and pressure. According to the Equation (5), the outlet temperature of station can be calculated.

2.4. Modeling the actual gas behavior at the pressure reduction station

From the microscopic viewpoint, an ideal gas has the equation of state as $Pv = RT$, but this equation is true if there is no molecular force like when the pressure is very low and the temperature is very high. However, in the range of working temperature and pressure of PRS, the assumption of ideal gas leads to errors in engineering calculations. Therefore, the actual gas behavior should be modeled in the range of working conditions.

According to the Equation (6), the enthalpy for real gas is a function of temperature and pressure:

$$h = h(T, P) \quad (6)$$

Therefore:

$$dh = \left(\frac{\partial h}{\partial T}\right)_P dT + \left(\frac{\partial h}{\partial P}\right)_T dP \quad (7)$$

And

$$Tds = dh - vdp \quad (8)$$

By differentiating from Equation (8), we have the following equations for pressure at a constant temperature:

$$\left(\frac{\partial h}{\partial p}\right)_T = v + T\left(\frac{\partial s}{\partial p}\right)_T \quad (9)$$

$$C_p = \left(\frac{\partial h}{\partial T}\right)_p \quad (10)$$

$$dG = vdp - sdT \quad (11)$$

By differentiating the Equation (11):

$$\left(\frac{\partial s}{\partial p}\right)_T = -\left(\frac{\partial v}{\partial T}\right)_p \quad (12)$$

By placing the Equations (9), (10) and (12) in Equation (7):

$$dh = C_p dT + \left[v - T\left(\frac{\partial v}{\partial T}\right)_P\right] dP \quad (13)$$

Equation (13) can be simplified in accordance with the Equation (14):

$$dh_T = \left[v - T\left(\frac{\partial v}{\partial t}\right)_P\right] dP \quad (14)$$

By integrating the Equation (14):

$$(h_{2-}h_1)_T = \int_1^2 \left[v - T\left(\frac{\partial v}{\partial T}\right)_P\right] dP \quad (15)$$

The main point about $(h_{2-}h_1)_T$ is that the change in enthalpy at constant temperature is a function of *P-V-T* behavior of gas. In other words, if the equation of state is known for a material, it is possible to change the enthalpy at a constant temperature by deriving and integrating. As the general diagram is a demonstration of *P-V-T* behavior of gas, this equation can be used to prepare a general diagram for the enthalpy change in an isothermal process [26]. Since the outlet temperature is unknown after the pressure reduction, the above idea can be utilized to determine this temperature. In order to be able to use equations of the ideal gas, it is necessary to reach the States 1* and 2* from States 1 and 2 respectively during the

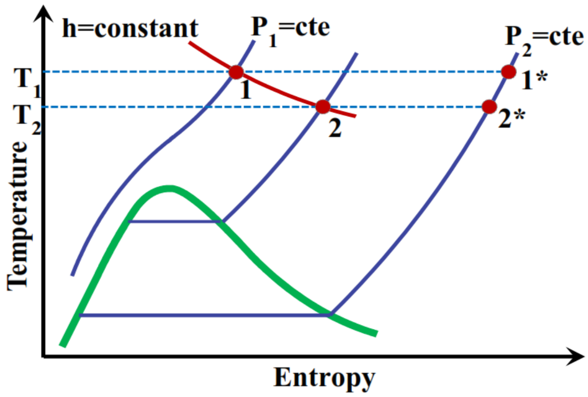

Figure 3. Determination of output unknown temperature (T_2)

constant temperature process in accordance with the Fig.3.

2.5. Software Code

An application, which was written in the MATLAB software environment and consisted of three parts, was used to facilitate the calculation of outlet temperature of a PRS. The first part consisted of receiving specified inputs and outputs of the natural gas PRS, physical properties of natural gas (methane), the input of PRS 1 of Semnan City (as a case study) with a heater according to Table 1. The second part consisted of the solution of equation of the first law of thermodynamics based on the enthalpy deviation and its repetition until the Equation (5) was satisfied according to the Equation (16) and in accordance with Fig. 3. The third part covered the calculation of outlet temperature.

$$-(h_1^* - h_1) + (h_1^* - h_2^*) + (h_2^* - h_2) = 0 \qquad (16)$$

The mean difference of results of measured and calculated temperatures can be determined using the Equation (17):

$$M.E.P = \frac{1}{n_d} \sum [\frac{T_{mea} - T_{est}}{T_{est}}] * 100 \qquad (17)$$

that *M.E.P* is the mean error percentage, n_d: is number of test days, T_{mea}: is measured temperature and T_{est}: is the calculated temperature by the software.

2.6. Uncertainty analysis

Experimental investigation is always accompanied by errors [30]. Therefore, researchers always try to minimize the amount of errors [31]. Owing to the accuracy of measuring and experimental instruments, there are limitations in this field . In the present study, the uncertainties of all the measured independent parameters are calculated and are presented in Table 2 [32].

It should be noted that, prior to the measurement, the accuracy of the measuring equipment performance was compared with valid calibrated samples, which were close to the reference values.

Table 1. Structural, thermal and fluids characteristics of heater [29].

Quantity	Value	Unit
inlet gas temperature	20	° C
natural gas mass flowrate	1556	kg/s
coil diameter	0.15	m
Coil Number	7	-
shell diameter	23.08	m
overall heat transfer coefficient	568	$W/m^2.K$
Water capacity inside the heater	23	m^3
Water temperature at instant t=0	50	° C
water density	1000	kg/m^3
Fire tube area	88.1	m^2
Fire tube overall heat transfer coefficient	568	$W/m^2.K$
average ambient temperature	15	° C

Table 2. The list of measuring properties, instruments, characteristics and their uncertainties.

Property	Company	Range	Unit	Accuracy	Uncertainty $(u = a/\sqrt{3})$
Inlet Temperature	Pakkens	0-120	°C	1	0.58
Outlet Temperature	InstruMate	0-150	°C	0.5	0.29
Inlet Pressure	WIKA	0-70	bar	1	0.58
Thermodynamic Properties: Enthalpy					0.1%

3. Results and discussion

3.1. Validation of results

In order to validate results and compare them with measured values at the Semnan gas PRS, the outlet temperature of 10 days was measured at a specified hour (18:00). To improve the accuracy of temperature measurement, a digital thermometer was used at the station output (after the regulator.- The results are presented in Table 3.

Based on results of Table 3, the mean difference of results of measured and calculated temperatures can be determined using the Equation (17). M.E.P is 9% indicating that calculations are close to measured values and by engineering judgment, this difference can be accepted. Fig.4 shows the results of the measured temperature and the calculated temperature within 10 days of testing at a given hour.

The heat capacity of the heaters is proportional to the capacity of the natural gas PRS. In order to increase the temperature of one cubic meter of gas to one degree centigrade, it requires 70 BTU of energy [7]. As shown in Table 4, during the operation of the heater for one year, 258,658,160 BTU (equal to 272,625,701 kJ per year) of heat is applied over the amount of gas needed.

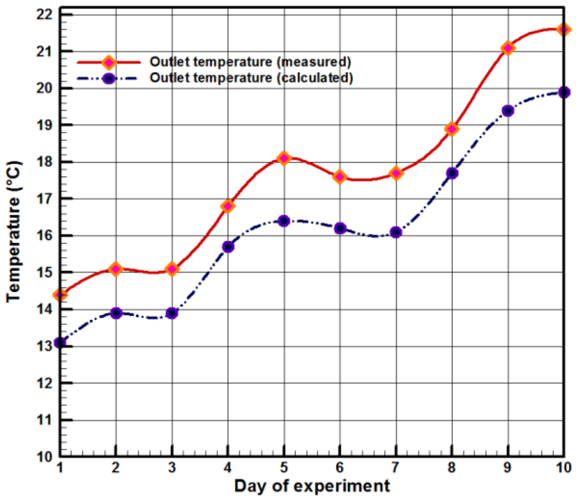

Figure 4. Results of output measured and calculated temperatures.

Table 3. Results of output measured and calculated temperatures according to definite input temperature, input and output pressures

date	Inlet pressure (MPa)	Outlet pressure (MPa)	Inlet temperature (°C)	Outlet temperature (°C) (measured)	Outlet temperature (°C) (calculated)	Error percentage between measured and calculated values
2018/11/28	3.20	1.7	20	14.4	13.1	9%
2018/11/30	3.40	1.7	21	15.1	13.9	8%
2018/12/01	3.47	1.7	21	18.2	16.5	9%
2018/12/03	2.86	1.7	21	16.8	15.7	7%
2018/12/04	3.74	1.7	25	18.1	16.4	10%
20181/2/09	3.26	1.7	24	17.6	16.2	9%
2018/12/12	2.79	1.7	22	17.7	16.1	9%
2018/12/15	3.53	1.7	23	18/9	17.4	7%
2018/12/17	3.49	1.7	22	21.1	19.4	9%
2018/12/19	2.79	1.7	26	21.6	19.9	9%

Table 4. The amount of excess heat applied to a gas during a year (natural gas PRS no.1 Semnan).

No.	month	Outlet gas temperature from PRS (°C)		Heater situation	Excess gas temperature value (compared to the standard temperature) (°C)	The amount of gas passing from PRS(SCMH)	Excess heat applied to the gas (BTU)
		The calculated value	The measured value				
1	Apr 2018	14	21	On	6	31,099	13061580
2	May 2018	17	17	Off	-	26,009	-
3	Jun 2018	17	17	Off	-	23,093	-
4	Jul 2018	20	20	Off	-	22,817	-
5	Aug 2018	19	19	Off	-	19,772	-
6	Sep 2018	17	17	Off	-	21,102	-
7	Oct 2018	14	23	On	8	33,113	15894240
8	Nov 2018	12	25	On	10	62,334	43633800
9	Dec 2018	9	26	On	11	70,436	54235720
10	Jan 2019	8	25	On	10	79,465	55625500
11	Feb 2019	12	23	On	8	87,452	48973120
12	Mar 2019	13	20	On	5	77,812	27234200

Low heating value (LHV) of natural gas input to the PRS no.1 of Semnan is 34147.68 kJ/SCM [33]. As a result, 7983.7 SCM of natural gas is consumed more than needed in a year. If this amount of energy saving (ES) is multiplied by the world price of natural gas (0.19 USD) [33], It can be seen that the annual benefit at only one natural gas PRS is about 1516.8 USD. Considering the total number of PRSs in our country, this amount of energy saving and financial benefits will increase significantly.

Obviously, even preventing a small part of the energy

Table 5. Emission factors of GHG for natural gas [36].

Fuel	Emission factor		
	CO_2	**CH_4**	**N_2O**
Natural gas	56.1×10^{-3}	10^{-6}	10^{-7}

waste will result in a large energy saving and preservation of national capital.

The natural gas industry has had a long history of mitigating methane emissions as greenhouse gas (GHG). Methane is the primary component of natural gas [34], and reductions of methane emissions are important for operational efficiency, safety, and environmental excellence. The reduction of GHG emissions from natural gas, due to utilization proposed control system in this research, can be determined using the Equation (18) [35]:

$$E_{c,NG,j} = ES_{NG} \times LHV \times EF_{NG,j} \tag{18}$$

Where:

$E_{c,NG,j}$ is the amount of mitigation GHG from natural gas combustion (tone)

j is GHG (CO_2, CH_4, N_2O)

ES_{NG} is the amount of energy saving (m^3)

LHV is low heating value of natural gas ($34.2 \times 10^{-3}\ GJ/m^3$).

$EF_{NG,j}$ is emission factor of j for natural gas which is calculated from Table 5.

By replacing above values in Equation (18), from emission 15.29 tone GHG , was prevented whithin a year, only in one PRS. Since GHG emissions cause environmental hazards and safety risks, reducing emission will have substantial economic and environmental benefits.

3.2. Suggested control system

The necessary heat for heater can be obtained with a good estimation by specifying the temperature of outlet gas from the natural gas PRS depending on the temperature of inlet gas. Considering the heater as the control volume, the continuity equation and the first law of thermodynamics are according to Equations (19) and (20) [26]:

$$\left(\frac{\mathrm{dm}}{\mathrm{dt}}\right)_{\mathrm{c.v.}} + \dot{m}_e - \dot{m}_i = 0 \tag{19}$$

$$\dot{Q}_{\mathrm{c.v.}} + \dot{W}_{\mathrm{c.v.}} = \left(\frac{\mathrm{dE}}{\mathrm{dt}}\right)_{\mathrm{c.v}} + \dot{m}_e\left(h + \frac{V^2}{2} + gz\right)_e - \dot{m}_i\left(h + \frac{V^2}{2} + gz\right)_i \tag{20}$$

Considering the steady flow regardless of kinetic and potential energy changes and axial work, the first law of thermodynamics is simplified as the Equations (21-a) and (21-b) [26]:

$$\dot{Q}_{\mathrm{c.v.}} = \dot{m}_e h_e - \dot{m}_i h_i \tag{21-a}$$

$$\dot{Q}_{\mathrm{c.v.}} = \dot{m}(h_e - h_i) \tag{21-b}$$

where, T_i is the inlet temperature (which can be measured) and Te is the outlet gas temperature (which is predicted). According to the Equation (22), mass flow rates are necessary to calculate the applied heat rate. Since the mass flow rate was not present on the information display device (pressure, temperature, and corrected volume) at the Dispatching Center of Semnan gas company and only the daily consumption of gas flow was recorded, the mass flow rate was calculated with a good approximation by obtaining daily consumption rate and values of standard pressure and temperature or T=288.15 K and P=101.305 kPa [6] according to the Equation (23):

$$\dot{m} = \frac{p\,\dot{v}}{R\,T} \tag{23}$$

As mentioned above, the heat is first given to the water which transmits the heat indirectly to the flowing gas. Therefore, this amount of heat should be applied to the water. The higher the flow rate of gas, the more energy is needed to raise the water temperature in the heater. The immersed natural gas flow in water could be considered as pipe in constant temperature environment [23]. Since the temperature of inlet gas of station is known and the temperature of outlet gas is predicted, the required water temperature ($\mathbf{T_w}$) can be calculated according to equation as below [37]:

$$e^Y = \frac{T_w - T_e}{T_w - T_i}, \qquad Y = \frac{-\pi D_{oc} L_c U_C}{\dot{m} C_P} \tag{24}$$

In the Equation (24), $\mathbf{T_w}$ is the water temperature; $\mathbf{T_i}$: Inlet gas temperature; $\mathbf{T_e}$: Outlet gas temperature; $\mathbf{D_{oc}}$: Outer coil diameter; $\mathbf{L_c}$: Length of coils; and $\mathbf{U_C}$: Total heat transfer coefficient of coil. $\mathbf{T_w}$ is unknown; $\mathbf{T_i}$ is measured, and $\mathbf{T_e}$ is calculated according to the Equation (16); and - other specifications are available in catalogs of manufacturing companies according to Table 1 and relevant handbook [38]. Rearranging the above equation and solving for $\mathbf{T_w}$, one could drive the following equation:

$$T_W = (T_e - T_i e^Y)/(1 - e^Y) \tag{24-a}$$

A schematic view of used equipment is represented in Fig. 5. The optimum gas temperature (sign 8), can be predicted by the outlet temperature (according to Equation (16)) and calculating the water heater temperature (sign 12) (according to the Equation (24-a)) by applying an solenoid valve (sign 14), in the heater fuel path and through a controlling mechanism (sign 11). The flowchart of suggested control system is shown in Fig. 6.

In other words, a digital thermostat is installed at the outlet of PRS, and when the gas temperature reaches the standard natural gas temperature, it gives the command of fuel flow disconnection to the solenoid valve on the path of fuel supply system heater. This method prevent the too much consumption of fuel for heating the flowing gas from the natural gas PRS and avoids the dissipation of a large amount of energy. It is worth mentioning, at the moment, owing to the lack of a control system, the temperature of outlet gas exceeds the standard temperature, and as a result, a lot of energy has been wasted. Fig. 7 shows images from demo installation.

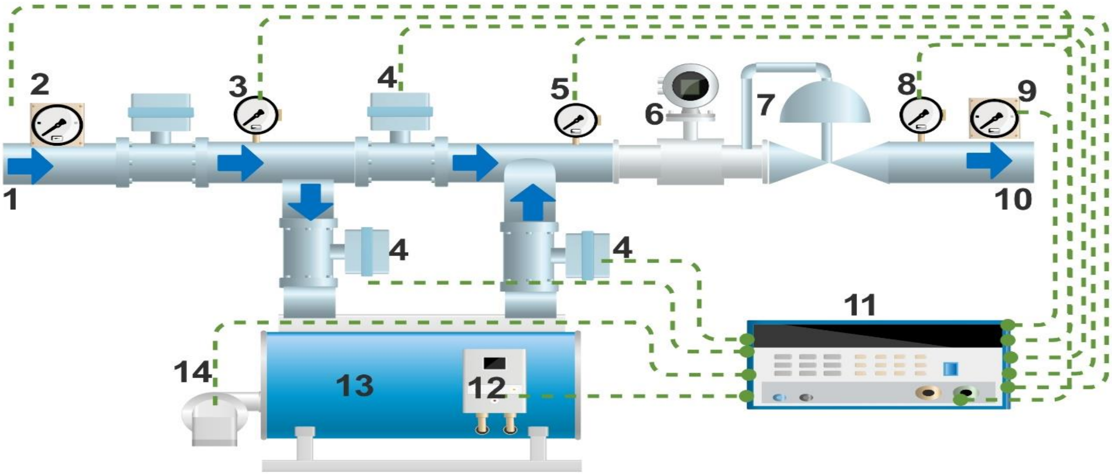

Figure 5. Schematic of control system for optimum output gas temperature: 1-inlet gas, 2-inlet gas temperature indicator, 3-inlet pressure gauge, 4-control valve, 5-midle pressure gauge, 6-gas flow meter, 7-regulator, 8-outlet pressure gauge, 9-outlet digital gas temperature indicator, 10-outlet gas, 11-controller, 12-water temperature sensor , 13-heater and 14-burner solenoid valve.

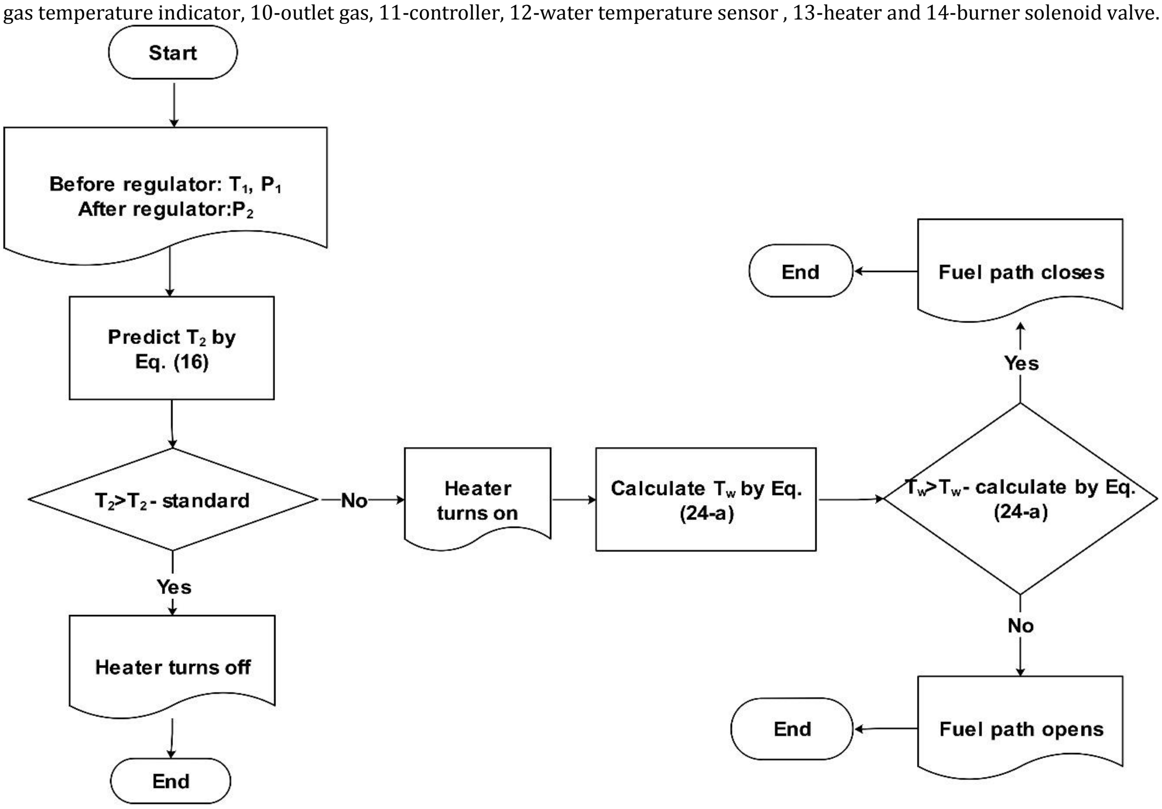

Figure 6. Flowchart of suggested control system

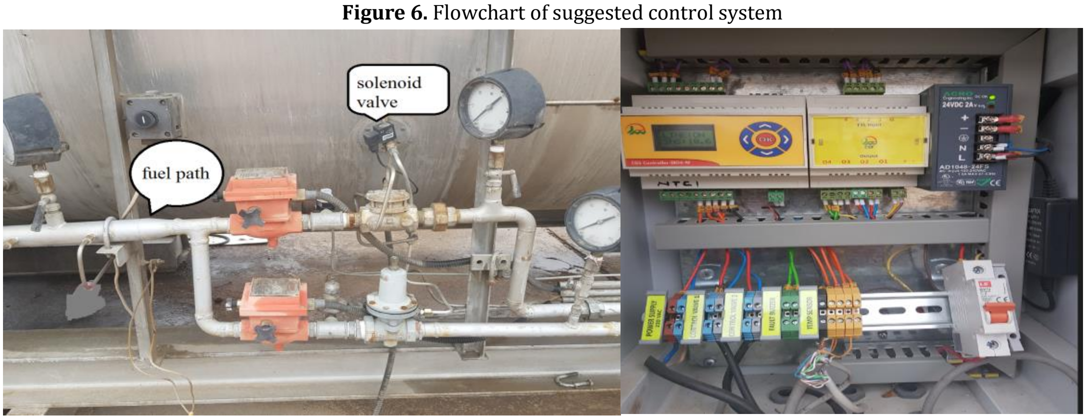

Figure 7. Use of solenoid valve and control system in the heater of PRS.

3.3. Economic analysis

The first annual cost of suggested control system, FAC, is obtained as [39–41]:

$$FAC = P \times CRF \tag{24}$$

where CRF and P indicate the capital recovery factor and the capital cost of the suggested control system, respectively. CRF is calculated as [39]:

$$CRF = i(1+i)^n/[(1+i)^n - 1] \tag{25}$$

where i and n denote the interest rate of lending banks and the life of the control system, respectively. Interest rate of lending banks equal to 20% is used for Iran (in the position of test). Moreover, the life of the control system is considered to be ten years. The annual salvage value (ASV) of the control system is determined by [39] :

$$ASV = SFF \times S \tag{26}$$

where S and SFF indicate the salvage value of the suggested control system and sinking fund factor, respectively. S is determined by [39]:

$$S = 0.2 \times P \tag{27}$$

SFF is defined as [39]:

$$SFF = i/[(1+i)^n - 1] \tag{28}$$

Annual maintenance cost, AMC, is determined as [39]:

$$AMC = 0.15 \times FAC \tag{29}$$

The total annual cost of the suggested system, is measured as [42]:

$$AC = FAC + AMC - ASV \tag{30}$$

The cost breakdown structure is presented in Table 6. As presented in this table, the total costs of the suggested system is 530 USD.

Table 7 presents the result of economic analysis. As presented in this table, the total annual cost of control system 141 is USD. Obviously, in the lifetime of the suggested control system, the capital cost is 1410 USD.

To evaluate the desirability and to investigate the cost effectiveness of the proposed system, the payback ratio has been calculated. The annual fuel saving and the capital cost are about 1516.8 USD and about 1410 USD respectively. Consequently, the payback ratio could be calculated as below:

$$payback\ ratio = \frac{capital\ cost}{annual\ benfit} = 0.93\ year \tag{31}$$

Table 6. Cost breakdown structure

Unit	No.	Cost($)
PLC	1	140
PLC power supply	1	80
Power supply:220/24	1	45
Electric board	1	16
Solenoid valve	1	25
Fuse, duct & terminal	The required number	14
Cable & fitting	The required number	30
Cost of implementation	-	180
Total		530

Table 7. Economic analysis of suggested control system.

P(USD)	S	n	i (%)	CRF
530	132.5	10	20	0.24
SFF	FAC	ASV	AMC	AC
0.04	127.2	5.3	19.1	141

Conclusion

A large capacity of the natural gas PRS is now used to heat gas during the heater operation (the cold months of year). Unfortunately, this amount of energy often exceeds the necessary amount to reach the standard gas temperature (15 ℃), and it has two major disadvantages: 1) Energy dissipation, 2) Damage to rubber parts in the PRS due to the thermal stress. Using the proposed method in this paper, the temperature of outlet gas of station was measured according to certain inlet pressure and temperature and the desired outlet pressure (1.7 MPa), so that the energy dissipation can be avoided with the knowledge about the outlet gas temperature using the proposed control system of this study. However, there was an average difference of 9% between the measured outlet temperature and calculated temperature by the software. The amount of energy saving and reduction of GHG emissions during a year at the PRS under studywere 7983.7 SCM and 15.29 tone, respectively. This method can largely prevent the energy dissipation at all natural gas PRSs. Even the avoidance of dissipation of a small portion of natural gas will obviously save a lot of energy in Iran. The payback period of implementation of this control system was estimated only less than one year. Since the effect of heavier hydrocarbons than methane was neglected in calculations, it is suggested considering their effects to increase the accuracy of results.

Nomenclature

a	Instrument accuracy
Cp	Specific heat (J/kg.K)
D	Diameter (m)
G	Gipps function
g	Gravity acceleration(m/s^2)
i	Interest rate (%)
L	Length(m)
m	mass(kg)
$\dot{m}$	mass flow rate (kg/s)
n	Life of the system (year)
p	Pressure(KPa)
P	Capital cost ($)
$\dot{Q}$	Heat transfer rate(J/s)
h	Enthalpy (J/kg)
R	Gas constant (J/kg.K)
s	Specific entropy (J/kg.K)

S	Salvage value ($)
T	Temperature (˚C)
t	Time(s)
U	Overall heat transfer coefficent(w/m^2 k)
u	Standard uncertainty
V	Velocity (m/s)
v	Specific volume(m^3/kg)
$\dot{w}$	Work rate(J/s)

Abbreviations

AC	Annual cost ($)
AMC	Annual maintenance cost ($)
ASV	Annual salvage value ($)
CRF	Cost recovery factor
EF	Emission factor
ES	Energy saving (m^3)
FAC	First annual cost ($)
GHG	Greenhouse gas
LHV	Low heating value (kJ/m^3)
MEP	Mean error percentage (%)
PRS	Pressure reduction station
SCM	Standard cubic meter
SFF	Sinking fund factor
USD	United states dollar

Subscripts

c.v.	Control volume
i	inlet
e	outlet

Greek symbols

μ	Joule–Thomson coefficient

Acknowledgements

The authors of paper are deeply grateful to the measurement and distibution departments of Semnan Gas Company and Energy and Sustainable Development Research Center, Semnan Branch, Islamic Azad University for providing necessary information and data for the present research.

References

[1] Zemansky, M.W., Abbott, M.M. and Van Ness, H.C., 1975. *Basic engineering thermodynamics*. McGraw-Hill Companies.

[2] Wu, M., Wang, S. and Liu, H., 2007. A study on inhibitors for the prevention of hydrate formation in gas transmission pipeline. *Journal of Natural Gas Chemistry*, *16*(1), pp.81-85.

[3] Gandhidasan, P., Al-Farayedhi, A.A. and Al-Mubarak, A.A., 2001. Dehydration of natural gas using solid desiccants. *Energy*, *26*(9), pp.855-868.

[4] Esmaeilzadeh, F., 2006. Simulation examines ice, hydrate formation in Iran separator centers. *Oil & gas journal*, *104*(11), pp.46-52.

[5] Rojey, A. and Jaffret, C., 1997. Natural gas production, processing, transport, Technip edition.

[6] Katz, C., Cornell, D., Kobayashi, R., Elenbaas, J.R. and Poettmann, F.H., 1959. WEINAUG, Handbook of Natural gas Engineering.

[7] ANSI/API Spec 12K, 1989. Indirect-Type Oil Field Heaters. 4th Edition.

[8] Shateri, M., Ghorbani, S., Hemmati-Sarapardeh, A. and Mohammadi, A.H., 2015. Application of Wilcoxon generalized radial basis function network for prediction of natural gas compressibility factor. *Journal of the Taiwan Institute of Chemical Engineers*, *50*, pp.131-141.

[9] Azizi, N., Rezakazemi, M. and Zarei, M.M., 2019. An intelligent approach to predict gas compressibility factor using neural network model. *Neural Computing and Applications*, *31*(1), pp.55-64.

[10] AGA8-DC92, E., 1992. Compressibility and super compressibility for natural gas and other hydrocarbon gases. *Transmission Measurement Committee Report*, (8).

[11] Erfani, A., Bahrami, A. and Varaminian, F., 2015. Processes and apparatuses for formation, separation, pelletizing storage and re-gasification of gas hydrate. *Journal of Heat and Mass Transfer Research*, *2*(2), pp.27-35.

[12] Rahbar, N., Shateri, M., Taherian, M. and Valipour, M.S., 2015. 2D Numerical Simulation of a Micro Scale Ranque-Hilsch Vortex Tube. *Journal of Heat and Mass Transfer Research*, *2*(1), pp.39-48.

[13] Falavand Jozaei, A., Tayebi, A., Shekari, Y. and Ghafouri, A., 2017. Numerical simulation of transient natural gas flow in pipelines using high order DG-ADER scheme. *Journal of Heat and Mass Transfer Research*, *4*(1), pp.35-43.

[14] Naderi, M., Ahmadi, G., Zarringhalam, M., Akbari, O. and Khalili, E., 2018. Application of water reheating system for waste heat recovery in NG pressure reduction stations, with experimental verification. *Energy*, *162*, pp.1183-1192.

[15] Zabihi, A. and Taghizadeh, M., 2016. Feasibility study on energy recovery at Sari-Akand city gate station using turboexpander. *Journal of Natural Gas Science and Engineering*, *35*, pp.152-159.

[16] Farzaneh-Gord, M., Ghezelbash, R., Arabkoohsar, A., Pilevari, L., Machado, L. and Koury, R.N.N., 2015. Employing geothermal

heat exchanger in natural gas pressure drop station in order to decrease fuel consumption. *Energy*, *83*, pp.164-176.

[17] Rezæi, M., Farzaneh-Gord, M., Arabkoohsar, A. and Dasht-bayaz, M.D., 2011, November. Reducing Energy Consumption in Natural Gas Pressure Drop Stations by Employing Solar Heat. In *World Renewable Energy Congress-Sweden; 8-13 May; 2011; Linköping; Sweden* (No. 057, pp. 3797-3804). Linköping University Electronic Press.

[18] Khosravi, M., Arabkoohsar, A., Alsagri, A.S. and Sheikholeslami, M., 2019. Improving thermal performance of water bath heaters in natural gas pressure drop stations. *Applied Thermal Engineering*, *159*, p.113829.

[19] Ashouri, E., Veysi, F., Shojaeizadeh, E. and Asadi, M., 2014. The minimum gas temperature at the inlet of regulators in natural gas pressure reduction stations (CGS) for energy saving in water bath heaters. *Journal of Natural Gas Science and Engineering*, *21*, pp.230-240.

[20] Rastegar, S., Kargarsharifabad, H., Shafii, M.B. and Rahbar, N., 2020. Experimental investigation of the increasing thermal efficiency of an indirect water bath heater by use of thermosyphon heat pipe. *Thermal Science*, 24(6B), pp.4277-4287.

[21] Khalili, E., Hoseinalipour, S.M. and Heybatian, E., 2011. Efficiency and heat losses of indirect water bath heater installed in natural gas pressure reduction station; evaluating a case study in Iran. In *The 8th National Energy Congress* (Vol. 24).

[22] Riahi, M., Yazdirad, B., Jadidi, M., Berenjkar, F., Khoshnevisan, S., Jamali, M. and Safary, M., 2011. Optimization of combustion efficiency in indirect water bath heaters of Ardabil city gate stations. In *Seventh Mediterranean Combustion Symposium (MCS-7)* (pp. 11-15).

[23] Farzaneh-Gord, M., Arabkoohsar, A., Dasht-bayaz, M.D. and Farzaneh-Kord, V., 2012. Feasibility of accompanying uncontrolled linear heater with solar system in natural gas pressure drop stations. *Energy*, *41*(1), pp.420-428.

[24] Olfati, M., Bahiraei, M., Heidari, S. and Veysi, F., 2018. A comprehensive analysis of energy and exergy characteristics for a natural gas city gate station considering seasonal variations. *Energy*, *155*, pp.721-733.

[25] Olfati, M., Bahiraei, M. and Veysi, F., 2019. A novel modification on preheating process of natural gas in pressure reduction stations to improve energy consumption, exergy destruction and CO2 emission: Preheating based on real demand. *Energy*, *173*, pp.598-609.

[26] Van Wylen, G.J. and Sonntag, R.E., 1967. Fundamentos de termodinámica (No. 536.7).

[27] Sanaye, S. and Nasab, A.M., 2012. Modeling and optimizing a CHP system for natural gas pressure reduction plant. *Energy*, *40*(1), pp.358-369.

[28] Shallcross, D.C., 2008. Psychrometric charts for water vapour in natural gas. *Journal of Petroleum Science and Engineering*, *61*(1), pp.1-8.

[29] H. Ken, Boiler Operator's Handbook. Fairmont Press, 2004.

[30] Bell, S., 2001. A Beginner's Guide to Uncertainty of Measurement, Issue 2. *Good practice guide*, (11).

[31] Kline, S.J., 1953. Describing uncertainty in single sample experiments. *Mech. Engineering*, *75*, pp.3-8.

[32] Dibaei, M. and Kargarsharifabad, H., 2017. New achievements in Fe3O4 nanofluid fully developed forced convection heat transfer under the effect of a magnetic field: An experimental study. *Journal of Heat and Mass Transfer Research*, *4*(1), pp.1-11.

[33] www.nigc.ir.

[34] Farzaneh-Gord, M., Pahlevan-Zadeh, M.S., Ebrahimi-Moghadam, A. and Rastgar, S., 2018. Measurement of methane emission into environment during natural gas purging process. *Environmental Pollution*, *242*, pp.2014-2026.

[35] Greenhouse Gases, 2006. Part 1: Specification with Guidance at the Organization Level for Quantification and Reporting of Greenhouse Gas Emissions and Removals. ISO 14064

[36] Van De Vate, J.F., 1997. Comparison of energy sources in terms of their full energy chain emission factors of greenhouse gases. *Energy Policy*, *25*(1), pp.1-6.

[37] Bergman, T.L., Incropera, F.P., Lavine, A.S. and Dewitt, D.P., 2011. *Introduction to heat transfer*. John Wiley & Sons.

[38] Arnold, K. and Stewart, M., 1999. *Surface production operations, Volume 2: Design of gas-handling systems and facilities* (Vol. 2). Elsevier.

[39] Esfahani, J.A., Rahbar, N. and Lavvaf, M., 2011. Utilization of thermoelectric cooling in a portable active solar still—an experimental study on winter days. *Desalination*, *269*(1-3), pp.198-205.

[40] Shoeibi, S., Rahbar, N., Esfahlani, A.A. and Kargarsharifabad, H., 2020. Application of simultaneous thermoelectric cooling and heating to improve the performance of a

solar still: An experimental study and exergy analysis. *Applied Energy*, *263*, p.114581.
[41] Kargar Sharif Abad, H., Ghiasi, M., Mamouri, S.J. and Shafii, M.B., 2013. A novel integrated solar desalination system with a pulsating heat pipe. *Desalination*, *311*, pp.206-210.
[42] Rastegar, S., Kargarsharifabad, H., Rahbar, N. and Shafii, M.B., 2020. Distilled water production with combination of solar still and thermosyphon heat pipe heat exchanger coupled with indirect water bath heater–Experimental study and thermoeconomic analysis. *Applied Thermal Engineering*, *176*, p.115437.